

Gaussian Splatting for Efficient Satellite Image Photogrammetry

Supplementary Material

Luca Savant Aira¹

Gabriele Facciolo²

Thibaud Ehret³

<https://mezzelfo.github.io/EOGS/>

¹ Politecnico di Torino, Corso Duca degli Abruzzi, 24, 10129 Torino TO, Italia

² Université Paris-Saclay, CNRS, ENS Paris-Saclay, Centre Borelli, 91190, Gif-sur-Yvette, France

³ AMIAD, Pôle Recherche, France

1. Additional visual results

We present additional visual results in Figs. 1 to 7.

2. Albedo and shadow visualization

We present in Figs. 8, 10 and 11 examples of albedos and shadows generated by EO-NeRF and the proposed EOGS for multiple scenes.

3. Details on the creation of the Sun Camera

Consider a view camera $\mathcal{A} : \mathbb{R}^3 \rightarrow \mathbb{R}^2, \mathbf{x} \mapsto A\mathbf{x} + \mathbf{a}$, the elevation function $\mathcal{E} : \mathbb{R}^3 \rightarrow \mathbb{R}, \mathbf{x} \mapsto \mathbf{e}^T \mathbf{x} + \Delta e$, and the sunlight direction $\mathbf{d} \in \mathbb{R}^3$ (available as elevation and azimuth from the dataset). Then the sun camera is $\mathcal{S} : \mathbb{R}^3 \rightarrow \mathbb{R}^2, \mathbf{x} \mapsto A(\mathbb{I}_3 - \frac{\mathbf{d} \otimes \mathbf{e}}{\mathbf{e}^T \mathbf{d}})\mathbf{x} + \mathbf{a}$.

4. Runtime details

The first line of Tab. 1 shows the number of views per scene, which is the same for all methods and ablations, hence it cannot be the source of EOGS speed.

The second line of Tab. 1 shows the number K_0 of Gaussians instanced at initialization. Note that the number of gaussians primitive K is non-increasing during the optimization, hence K_0 is also the peak number of Gaussians (and the peak memory usage $\approx 10\text{GB}$). As the scene volumes differ, we advocate to set $K_0 = 0.13V$, where V is the volume of the scene, such that a bigger scene, having more objects, has more Gaussians to represents them. The value of 0.13 was found experimentally, as a good trade-off between speed and reconstruction quality.

Scene (JAX/IARPA)	004	068	214	260	001	002	003
#views	8	16	20	14	24	20	21
$K_0 [10^6]$	0.40	1.00	2.27	0.67	0.93	1.47	1.47

Table 1

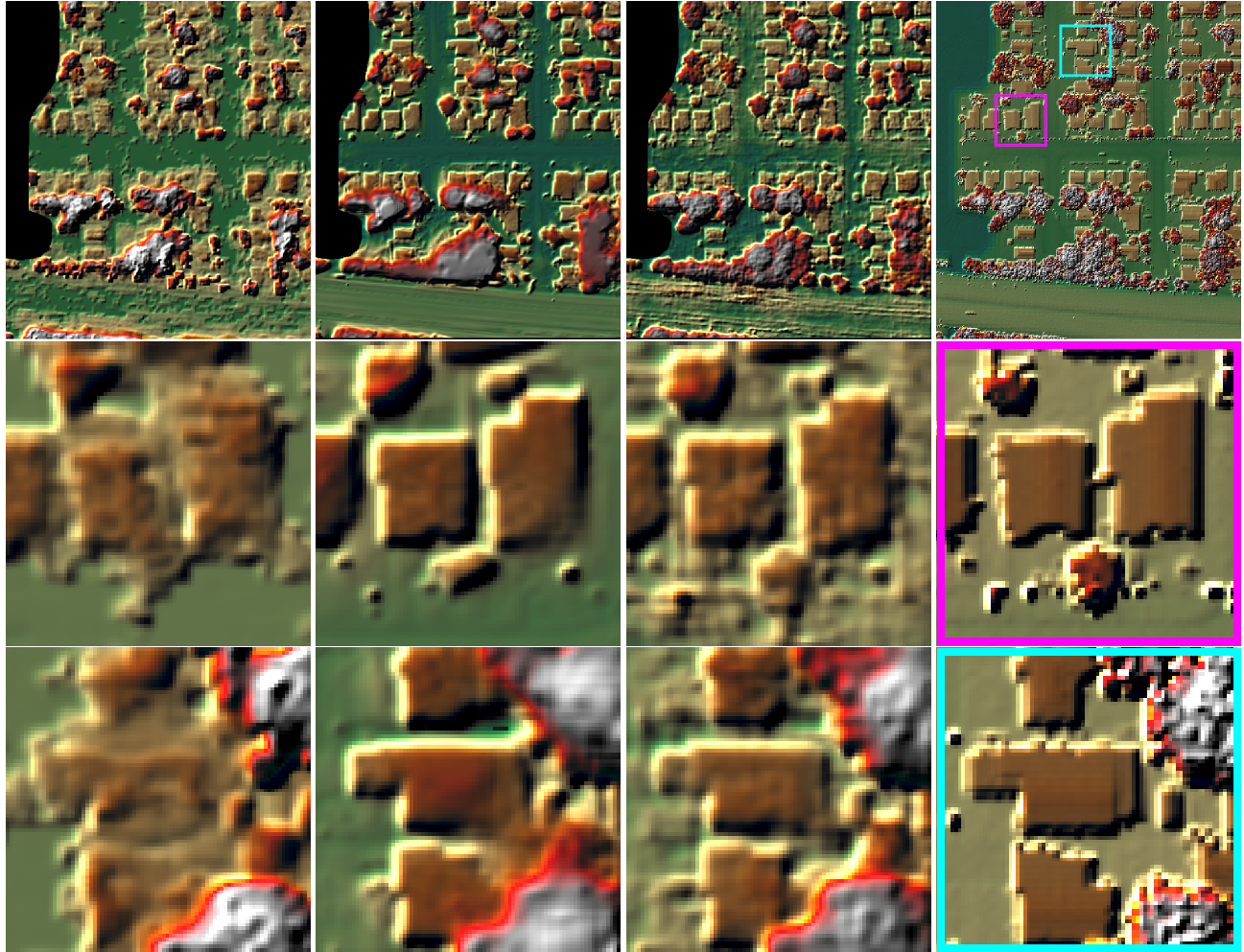


Figure 1. From left to right: visual results on JAX_004 comparing SAT-NGP [1], EO-NeRF [2] and the ground truth.

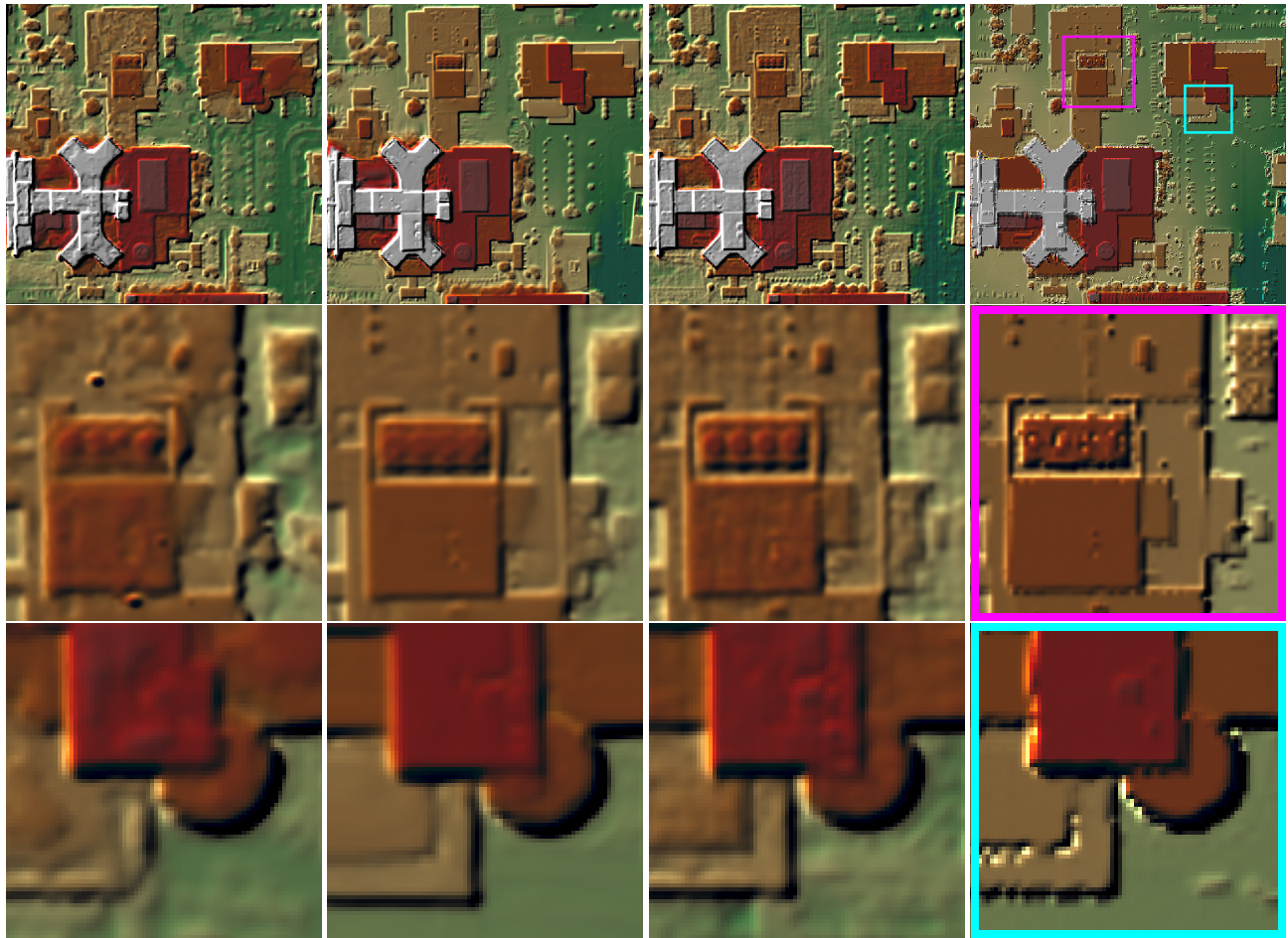


Figure 2. From left to right: visual results on JAX_068 comparing SAT-NGP [1], EO-NeRF [2] and the ground truth.

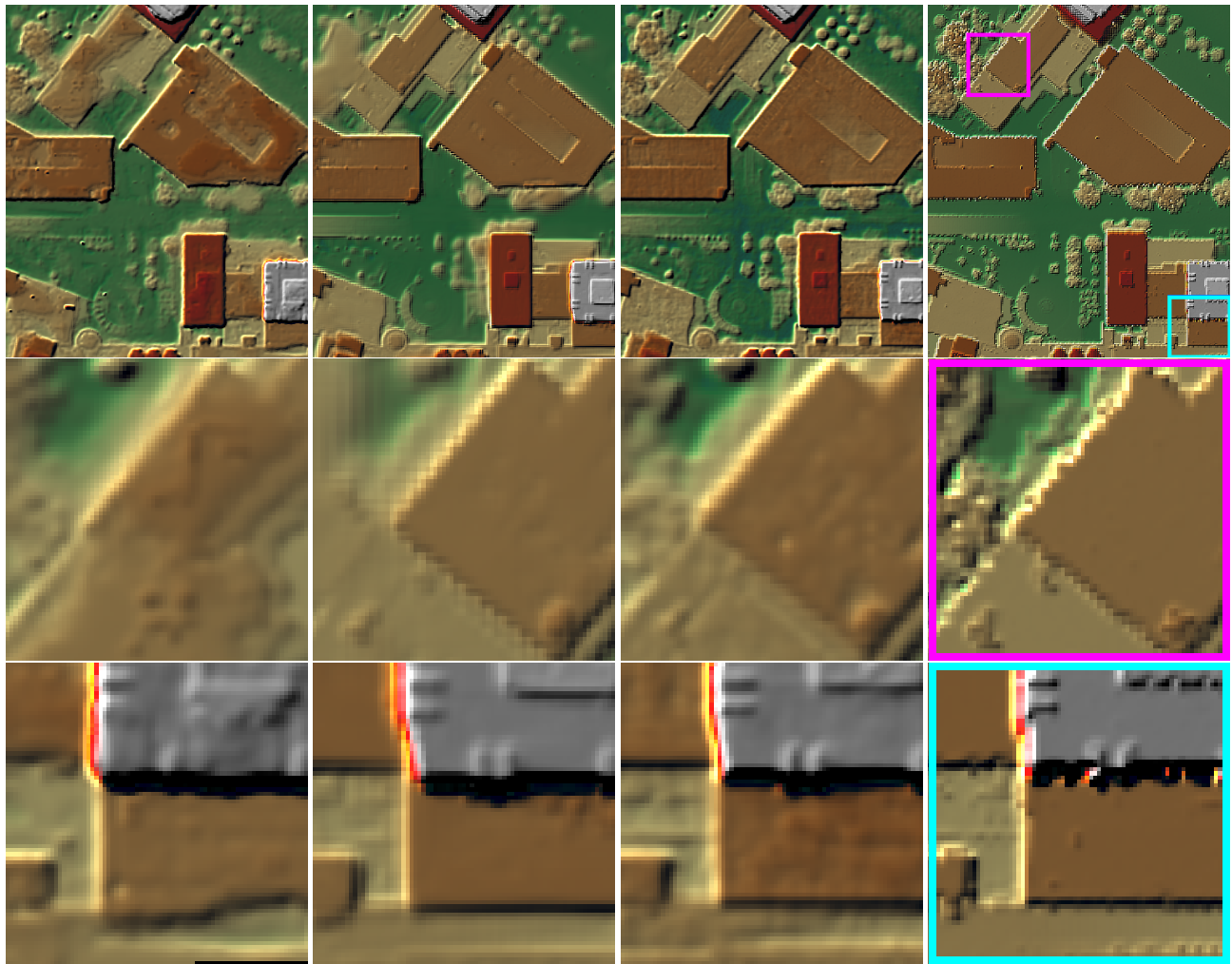


Figure 3. From left to right: visual results on JAX_214 comparing SAT-NGP [1], EO-NeRF [2] and the ground truth.

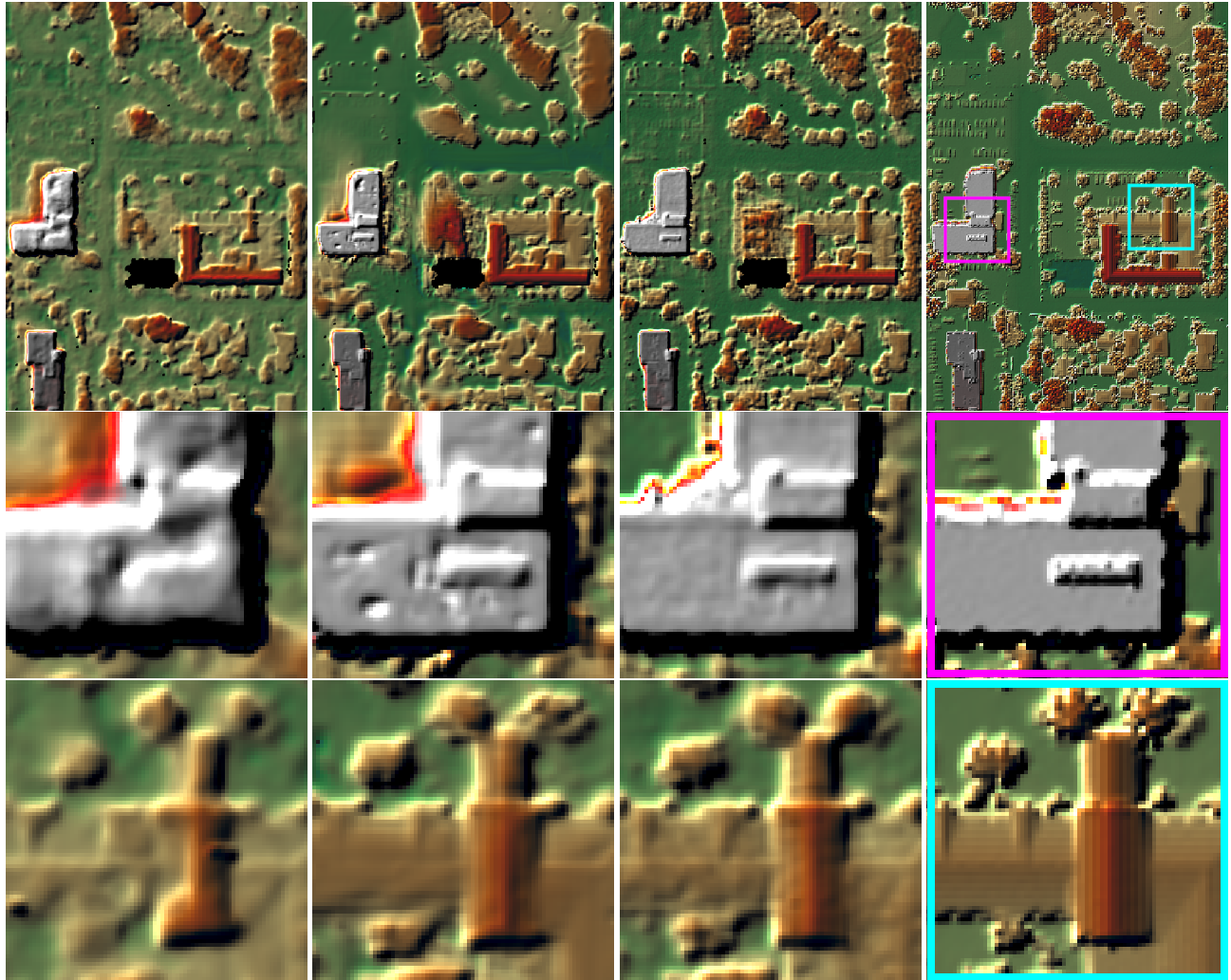


Figure 4. From left to right: visual results on JAX_260 comparing SAT-NGP [1], EOOGS, EO-NeRF [2] and the ground truth.

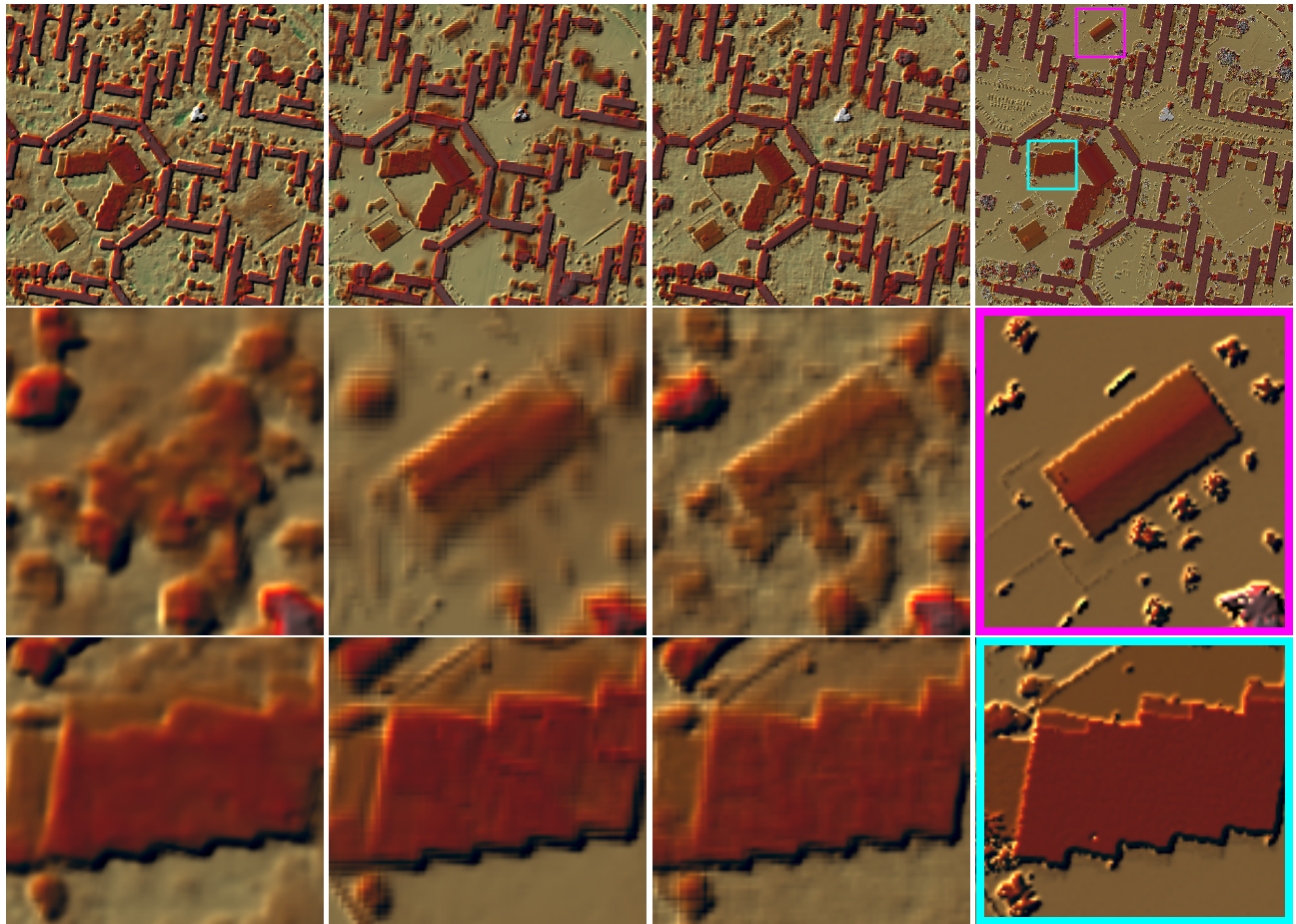


Figure 5. From left to right: visual results on IARPA_001 comparing SAT-NGP [1], EOOGS, EO-NeRF [2] and the ground truth.

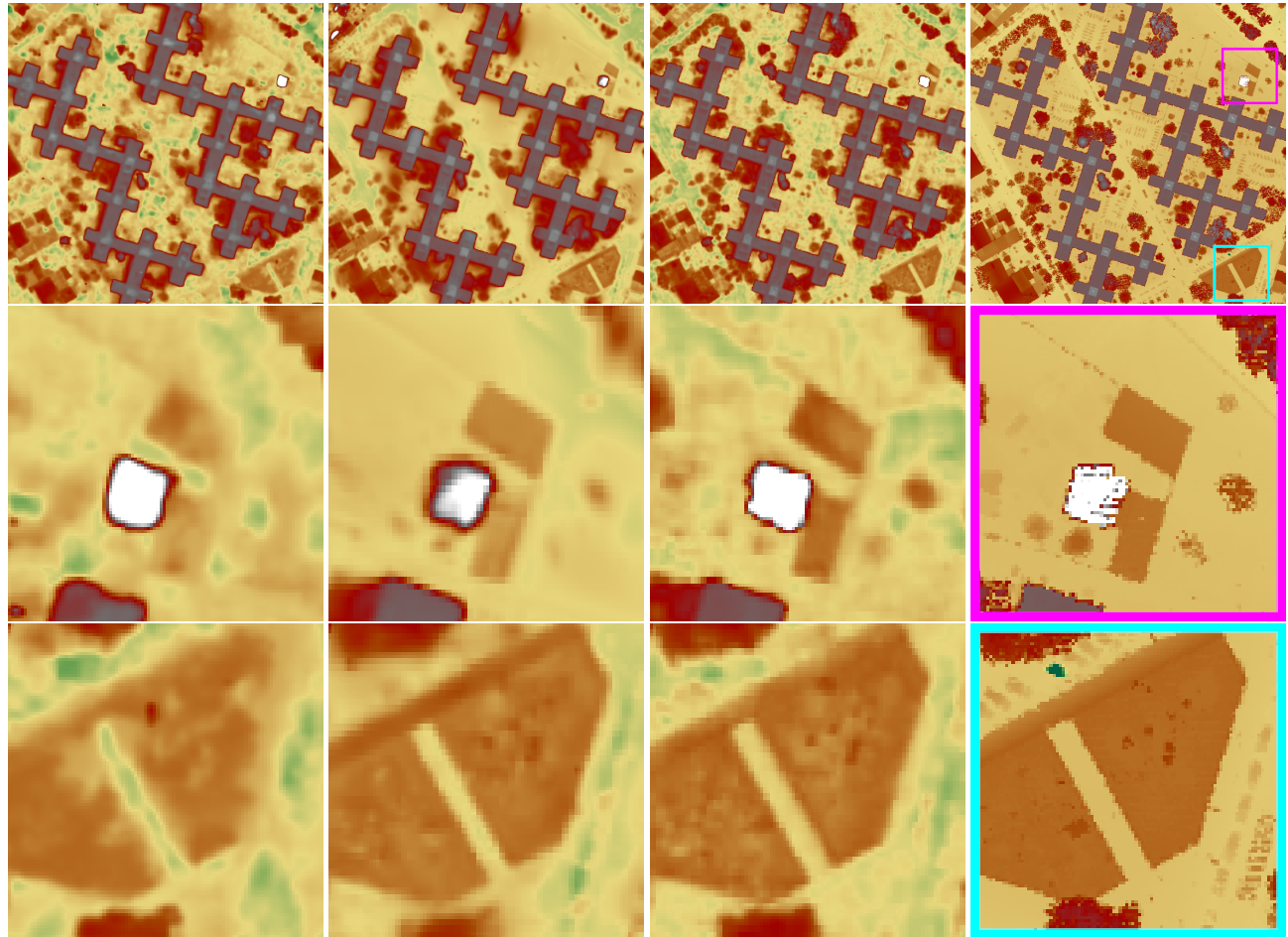


Figure 6. From left to right: visual results on IARPA_002 comparing SAT-NGP [1], EOGS, EO-NeRF [2] and the ground truth.

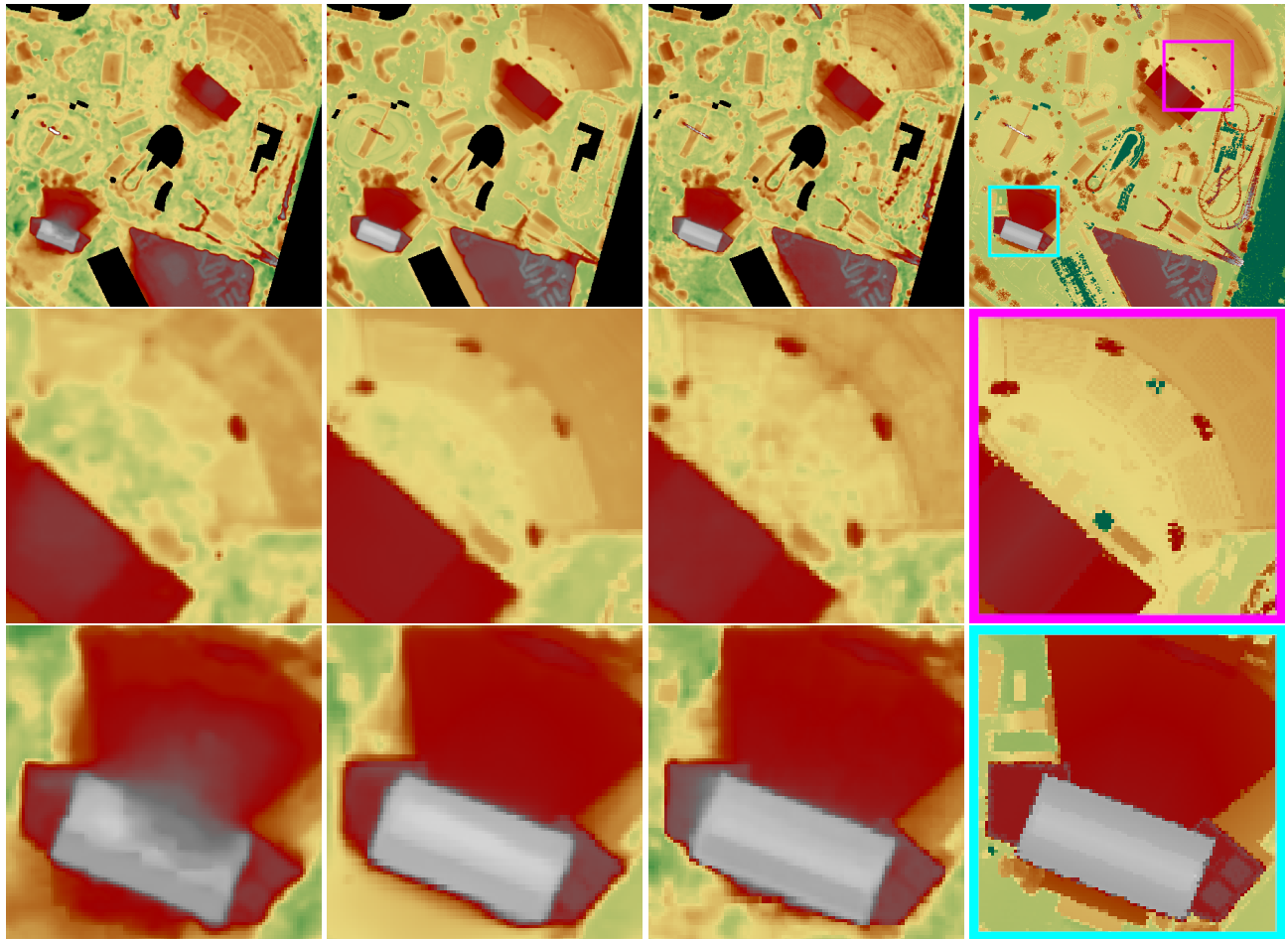


Figure 7. From left to right: visual results on IARPA_003 comparing SAT-NGP [1], EOOGS, EO-NeRF [2] and the ground truth.

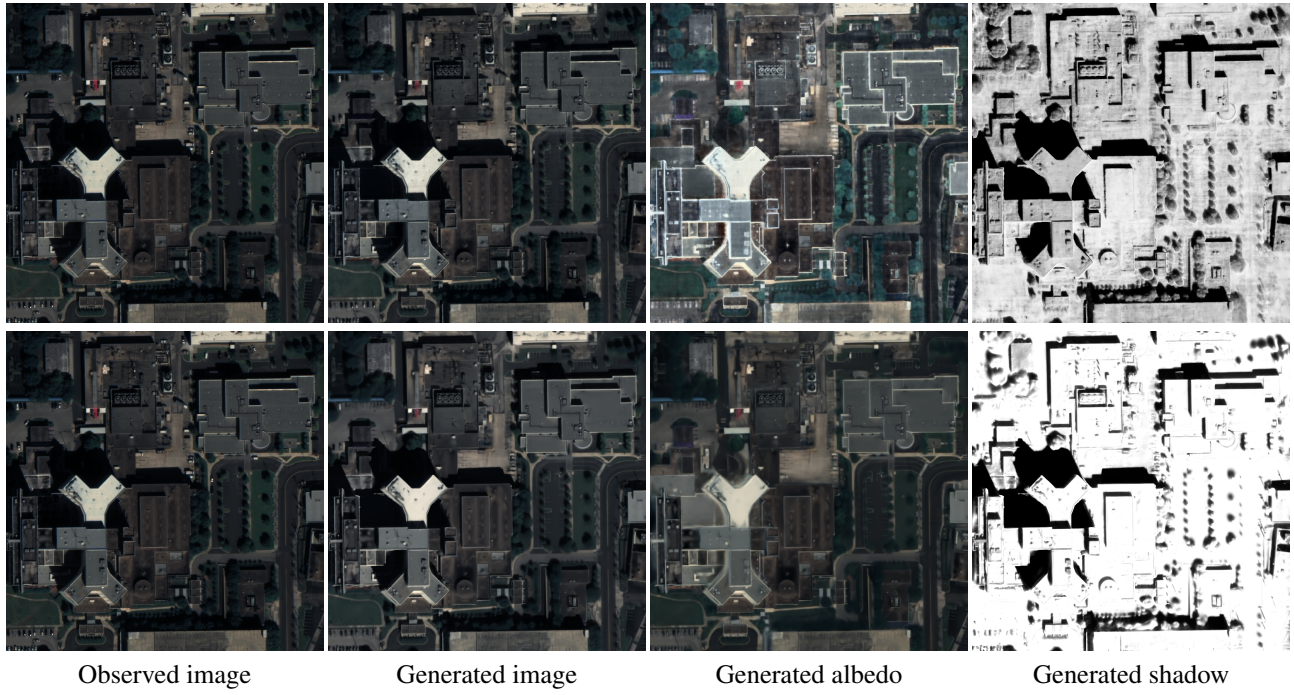


Figure 8. Visual comparison of the scene albedo and shadows generated by EO-NeRF (top) and EOOGS (bottom) for JAX_068. Note that the scaling for all images is the same except for the albedo that is rescaled independently to show the entire dynamic.

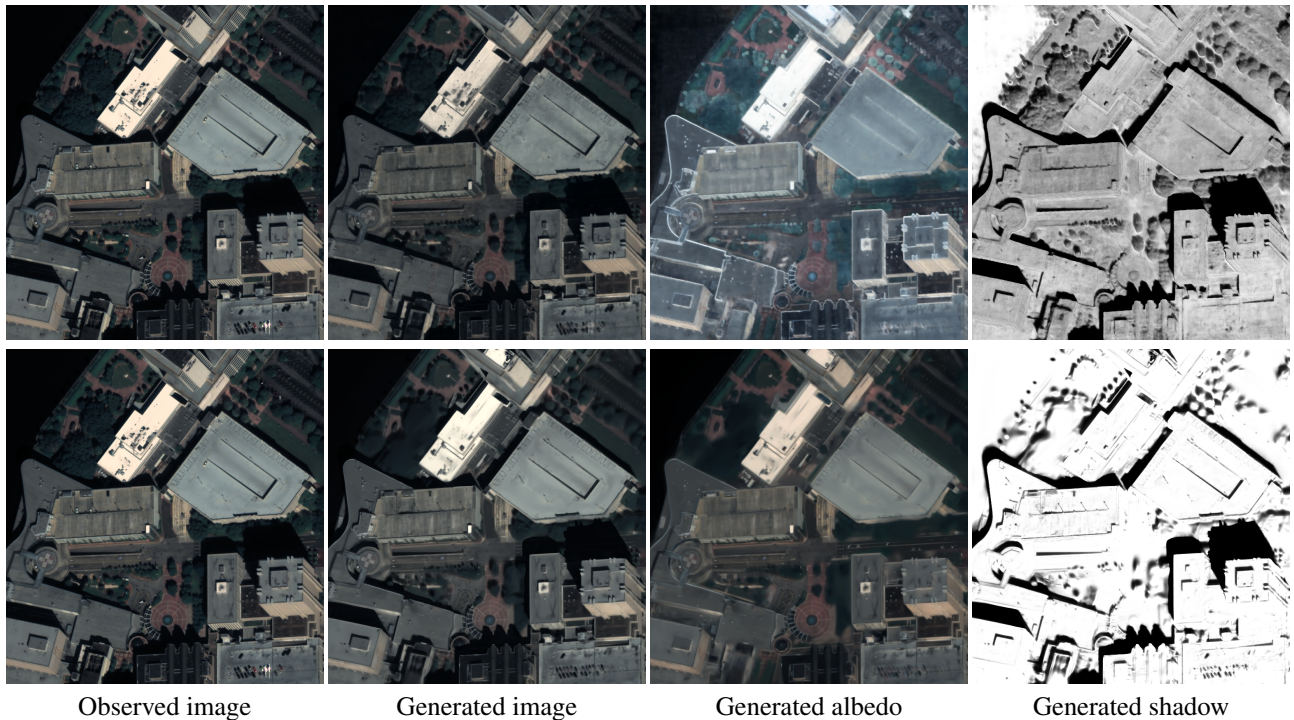


Figure 9. Visual comparison of the scene albedo and shadows generated by EO-NeRF (top) and EOOGS (bottom) for JAX_214. Note that the scaling for all images is the same except for the albedo that is rescaled independently to show the entire dynamic.

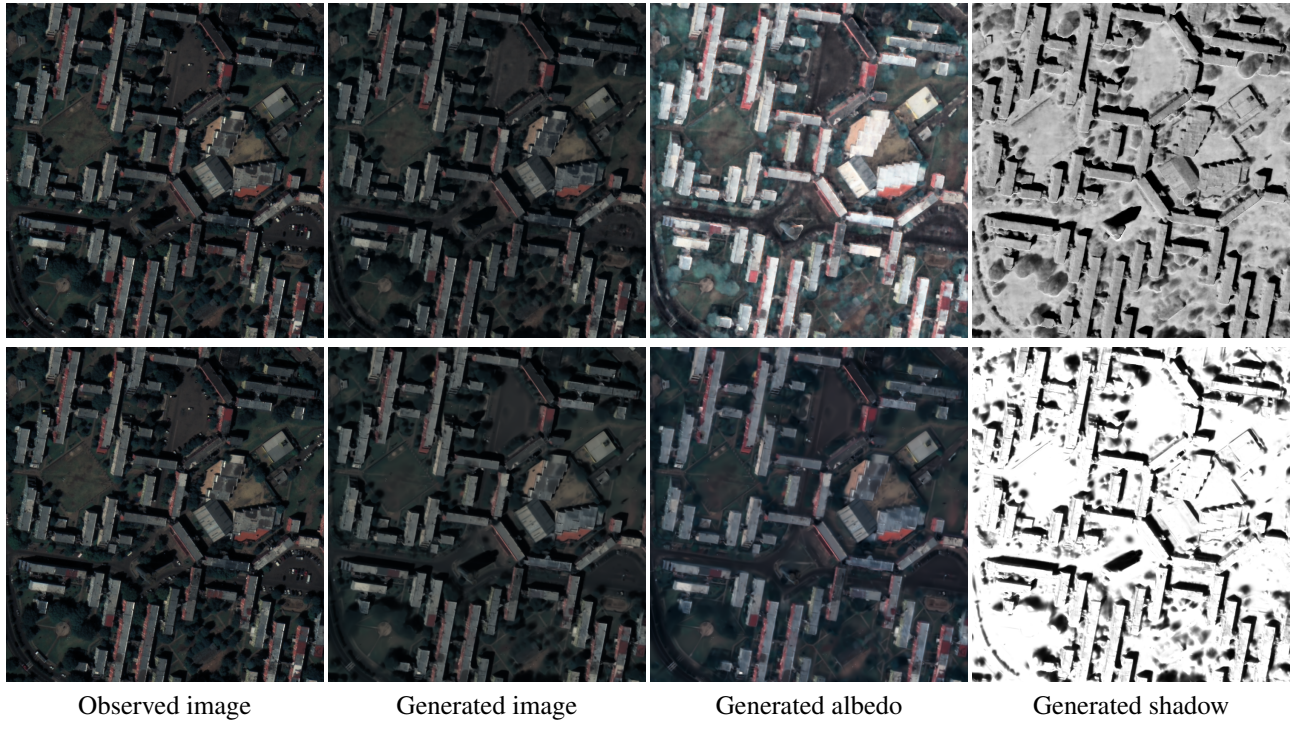


Figure 10. Visual comparison of the scene albedo and shadows generated by EO-NeRF (top) and EOOGS (bottom) for IARPA_001. Note that the scaling for all images is the same except for the albedo that is rescaled independently to show the entire dynamic.

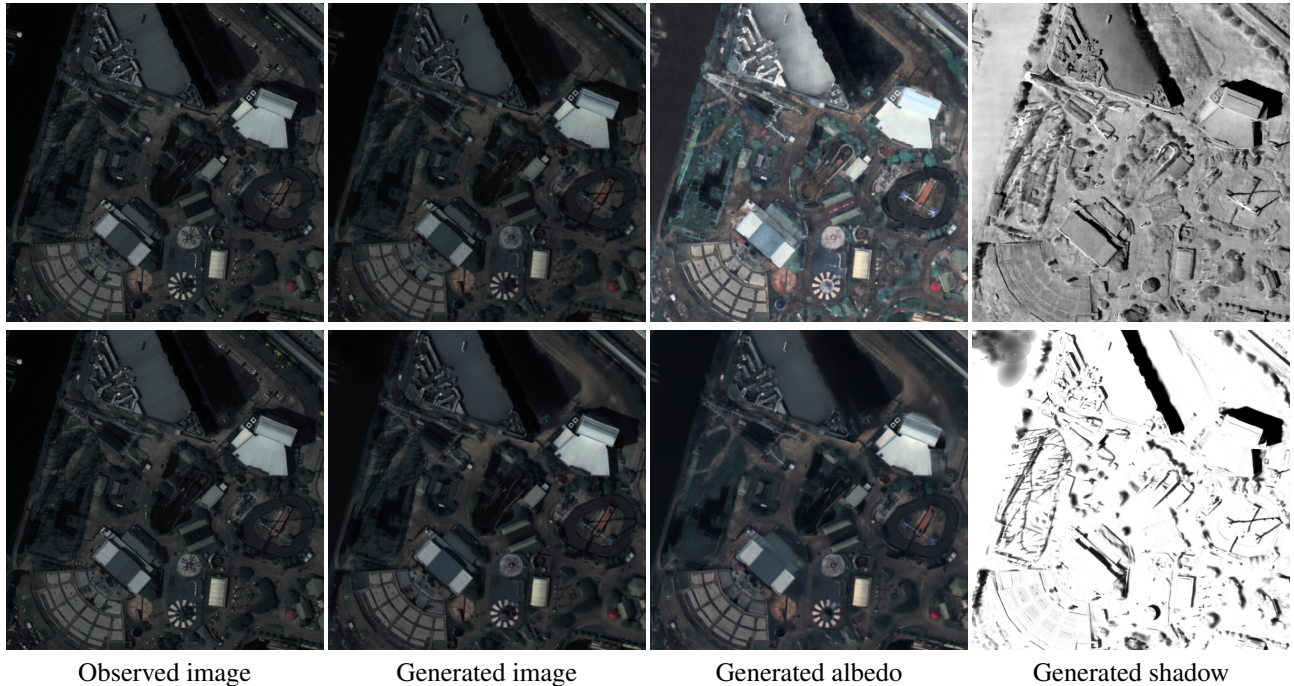


Figure 11. Visual comparison of the scene albedo and shadows generated by EO-NeRF (top) and EOOGS (bottom) for IARPA_003. Note that the scaling for all images is the same except for the albedo that is rescaled independently to show the entire dynamic.

References

- [1] Camille Billouard, Dawa Derksen, Emmanuelle Sarrazin, and Bruno Vallet. Sat-ngp : Unleashing neural graphics primitives for fast relightable transient-free 3d reconstruction from satellite imagery. In *IGARSS 2024 - 2024 IEEE International Geoscience and Remote Sensing Symposium*, pages 8749–8753, 2024. [2](#), [3](#), [4](#), [5](#), [6](#), [7](#), [8](#)
- [2] Roger Marí, Gabriele Facciolo, and Thibaud Ehret. Multi-date earth observation nerf: The detail is in the shadows. In *Proceedings of the IEEE/CVF Conference on Computer Vision and Pattern Recognition*, pages 2035–2045, 2023. [2](#), [3](#), [4](#), [5](#), [6](#), [7](#), [8](#)